



# Population Genetics of the São Tomé Caecilian (Gymnophiona: Dermophiidae: *Schistometopum thomense*) Reveals Strong Geographic Structuring

Ricka E. Stoelting<sup>1,2\*</sup>, G. John Measey<sup>3</sup>, Robert C. Drewes<sup>1</sup>

**1** Department of Herpetology, California Academy of Sciences, San Francisco, California, United States of America, **2** Department of Forest and Wildlife Ecology, University of Wisconsin, Madison, Wisconsin, United States of America, **3** Centre for Invasion Biology, Department of Botany and Zoology, University of Stellenbosch, Stellenbosch, South Africa

## Abstract

Islands provide exciting opportunities for exploring ecological and evolutionary mechanisms. The oceanic island of São Tomé in the Gulf of Guinea exhibits high diversity of fauna including the endemic caecilian amphibian, *Schistometopum thomense*. Variation in pigmentation, morphology and size of this taxon over its c. 45 km island range is extreme, motivating a number of taxonomic, ecological, and evolutionary hypotheses to explain the observed diversity. We conducted a population genetic study of *S. thomense* using partial sequences of two mitochondrial DNA genes (ND4 and 16S), together with morphological examination, to address competing hypotheses of taxonomic or clinal variation. Using Bayesian phylogenetic analysis and Spatial Analysis of Molecular Variance, we found evidence of four geographic clades, whose range and approximated age (c. 253 Kya – 27 Kya) are consistent with the spread and age of recent volcanic flows. These clades explained 90% of variation in ND4 ( $\rho_{CT}=0.892$ ), and diverged by 4.3% minimum pairwise distance at the deepest node. Most notably, using Mismatch Distributions and Mantel Tests, we identified a zone of population admixture that dissected the island. In the northern clade, we found evidence of recent population expansion (Fu's  $F_s = -13.08$  and Tajima's  $D = -1.80$ ) and limited dispersal (Mantel correlation coefficient = 0.36,  $p = 0.01$ ). Color assignment to clades was not absolute. Paired with multinomial regression of chromatic data, our analyses suggested that the genetic groups and a latitudinal gradient together describe variation in color of *S. thomense*. We propose that volcanism and limited dispersal ability are the likely proximal causes of the observed genetic structure. This is the first population genetic study of any caecilian and demonstrates that these animals have deep genetic divisions over very small areas in accordance with previous speculations of low dispersal abilities.

**Citation:** Stoelting RE, Measey GJ, Drewes RC (2014) Population Genetics of the São Tomé Caecilian (Gymnophiona: Dermophiidae: *Schistometopum thomense*) Reveals Strong Geographic Structuring. PLoS ONE 9(8): e104628. doi:10.1371/journal.pone.0104628

**Editor:** William J. Etges, University of Arkansas, United States of America

**Received:** November 4, 2013; **Accepted:** July 15, 2014; **Published:** August 29, 2014

**Copyright:** © 2014 Stoelting et al. This is an open-access article distributed under the terms of the Creative Commons Attribution License, which permits unrestricted use, distribution, and reproduction in any medium, provided the original author and source are credited.

**Funding:** The authors thank the European Commission Marie Curie Fellowship (HPMF-CT-2001-01407, field work support for GJM), the G. Lindsay Field Research Fund of the California Academy of Sciences (field work support for RES and RCD in 2001), and the Hagey Research Investment Fund of the California Academy of Sciences (field work support for RCD in 2006). The funders had no role in study design, data collection and analysis, decision to publish, or preparation of the manuscript.

**Competing Interests:** The authors have declared that no competing interests exist.

\* Email: stoelting@wisc.edu

## Introduction

Islands are self-contained natural laboratories and provide the backdrop to many of Darwin's and Wallace's observations that culminated in the theory of evolution [1]. Continuing in this role, they provide contemporary biologists with the opportunity to investigate ecological and evolutionary mechanisms [2–8]. On truly oceanic islands, isolation and competition for open ecological niches promote speciation [6], placing these locales in a prominent role when considering conservation of biodiversity [9]. In this context, the use of molecular phylogenetics has elucidated insular taxonomic relationships, providing insight into the mechanisms of island colonization and ecological radiations [10,11]. Many studies looking at insular species have concentrated on the examination of taxonomic relationships between islands [12–14], but, with their wealth of endemics, islands also provide an opportunity to study intraspecific population-level relationships in great detail.

Notable for its high endemism in both flora and fauna – including approximately 80 plants [15], 17–18 butterflies [16], 17 birds [17], 14 reptiles and five amphibians (RCD *pers. obs.* 1 Aug 2012) – São Tomé is one of three oceanic islands in the Gulf of Guinea that rose along the Cameroon Line roughly 13 Mya [18–19], and the largest at 836 km<sup>2</sup>, with the highest peak at 2024 m. Over the course of its existence, volcanic activity has reshaped topography [20–21] with recent data showing that it was active throughout the Pleistocene [19], likely contributing to the diversity observed; most recent flows have been placed between 0.85 and 0.03 Mya [19]. In addition, multiple independent colonization events have contributed to diversity, evidenced by phylogenetic relationships of geckos [22–23], skinks [24], and multiple snake species [25] on São Tomé and nearby islands.

The presence of salt-intolerant taxa on truly oceanic islands has garnered particular interest because mechanisms accounting for presence imply dispersal across marine environments, but direct dispersal is assumed to be limited by physiology. However, recent

phylogenetic studies have suggested the existence of delivery mechanisms, in particular oceanic currents, which carry flotsam [26–29], as well as the importance of decreased salinity of surface waters [27]. Such studies imply that colonization may be more common than previously assumed [30]. Here, we focus on an insular taxon of the sparsely-documented amphibian Order Gymnophiona – *a.k.a.*, caecilians – for which very little intraspecific information exists [31].

The caecilian amphibian *Schistometopum thomense* (Barboza du Bocage) [32] is a biogeographical enigma as it is endemic to the oceanic island of São Tomé, 225 km off the western coast of continental Africa, while its lone congener, *Schistometopum gregorii*, occurs on the far eastern coast of continental Africa (Kenya and Tanzania) [33]. Until recently, three endemic caecilian species were recognized from São Tomé, their differences based principally on coloration and head morphology. Presence of purple-brown flecking and a more pointed head shape differentiated *Schistometopum ephale* Taylor [34] from *S. thomense* (photographs, Figure 1). And, *Schistometopum brevirostre* (Peters) [35] was distinguished by Taylor [34] for its pale bluish coloration and slightly differentiated morphometric characters. But, subsequent morphological analyses suggested this division to be erroneous [36]; Nussbaum and Pfreder [36] synonymized all species to *S. thomense*, recognizing that criteria used to designate *S. ephale* Taylor were expressions of sexual dimorphism and of possible clinal variation from north to south on the island, and confirming that the third taxon – *S. brevirostre* – had been described without knowledge of the initial description [36–37]. Nevertheless, Nussbaum and Pfreder [36] found the range in color variation across this small island to be extreme and suggested limited dispersal ability for these caecilians as an explanation. The hypothesis that *S. thomense* may have limited dispersal ability receives further support from the finding that this species exhibits Bergmann's rule; Measey and Van Dongen [38] found that body mass doubled and length increased by nearly 50% along a 1,000 m elevational transect. Because subterranean organisms usually do not broadcast their biological parameters through morphology or easily-observable ecological niches, many questions remain about their taxonomy and ecology. For *S. thomense*, examining genetic variation at the species level offers indirect means to understand microevolutionary processes acting within this fossorial species.

In order to assess population structuring of *S. thomense*, we investigated the distribution of genetic diversity using mitochondrial DNA (mtDNA). In particular, we were interested in whether previously proposed taxonomic (i.e., multiple lineages) or clinal variation (i.e., one lineage) hypotheses could better explain the high phenotypic variation exhibited by caecilians on São Tomé [34,36,38]. In addition, we approximated the time to most recent common ancestor (MRCA) of lineages, thereby allowing investigation of the possibility that vicariant events contributed to the apparent diversity among caecilians on the island. As noted by Seyahooei et al. [39], maternally-inherited mitochondrial markers have the capacity to reflect female migration patterns that may be obscured in nuclear DNA (nDNA), which is subject to recombination. Thus, if distinct lineages led to the diversity of caecilians observed on São Tomé, we would expect to see a statistically-supported substructure of population groupings across the island. However, if clinal variation led to this diversity, we would expect subtler differentiation, with genetic distances between populations more closely mirroring geographic distance on São Tomé. If vicariant events had influenced intra-specific structure, we might expect that dates to MRCA and genetic structure correlate with estimated dates and breadth of volcanic activity and sea level

change – the only vicariant events for which we have data – on the island.

## Methods

### Ethics statement

Permission to collect, sample and export *Schistometopum thomense* on the island of São Tomé was granted by Hon. Arlindo Carvalho, Director General, Ministry of Environment, Republic of São Tomé and Príncipe. Ethics clearance for this study was granted by the Office for the Protection of Human and Animal Subjects, San Francisco State University (Protocol # A3-014).

### Study species

*Schistometopum thomense* (Barboza du Bocage) is an elongate, limbless, burrowing amphibian of the Order Gymnophiona (Dermophiidae, formerly Caeciliidae [40]), generally regarded as endemic to the island of São Tomé, though also represented by one specimen purportedly collected in the Ruwenzori region of the Democratic Republic of the Congo [36]. Adults range in total length from roughly 130 to 375 mm [36,38] and exhibit viviparous reproduction that is not tied to water [36]. These caecilians are one of only a few species that have been bred in captivity and, therefore, have a known age of maturity: 2 years [41]. This caecilian has received disproportionate attention amongst gymnophionans due to its striking yellow coloration and the relative ease with which it can be found, frequenting a variety of habitats from sea level to 1440 m in elevation [36,38,41–47]. Unflecked morphs appear more common in the north of the island and heavily flecked morphs appear more common in the south of the island, although geographic assignment of morphotype is not absolute [36,41–44,47]. We found these caecilians to be locally abundant [48], but impacts of land-use change [49] and recent entry into the pet-trade [50] on range and density are unknown.

### Sample collection

In order to assess genetic and chromatic variation within the range of *Schistometopum thomense*, we took photographs of and collected liver tissue from 138 specimens representing 24 geographic locales (“populations”) on the island of São Tomé (Figure 1). Specimens were deposited in the collections of the California Academy of Sciences' Department of Herpetology (CAS), the British Museum of Natural History (BMNH) and of author GJM (Table S1). Specimen collection dates encompass 2000 to 2006. Collection localities span the island, but reflect accessible habitat rather than the complete distribution of these animals. Liver tissue of *Schistometopum gregorii* (MW 03231) was used as an outgroup in phylogenetic analyses.

### Molecular data

Whole genomic DNA was extracted from liver tissue, using either phenol-chloroform [51] or DNeasy (Qiagen Inc., Valencia, CA) extraction protocols. From these samples, approximately 900 base pairs of NADH dehydrogenase subunit 4 (ND4) and associated tRNAs (histidine, serine and partial leucine) were amplified using the primers ND4 and Leu [52] in 100  $\mu$ L and 10  $\mu$ L reactions by hot-start PCR [51] and non-hot-start methods, respectively. Hot-start reactions were conducted in 100  $\mu$ L volumes (25  $\mu$ L Top Mix: 2 $\times$  buffer, 0.8 mM dNTPs, 1  $\mu$ M each primer; 75  $\mu$ L Bottom Mix: 0.67 $\times$  buffer, 2 mM MgCl<sub>2</sub>, 0.033 U Bioline Taq, 10  $\mu$ L template DNA), and used the temperature profile: 94°C for 7 min., 40 cycles of 94°C for 30 sec., 46°C–50°C

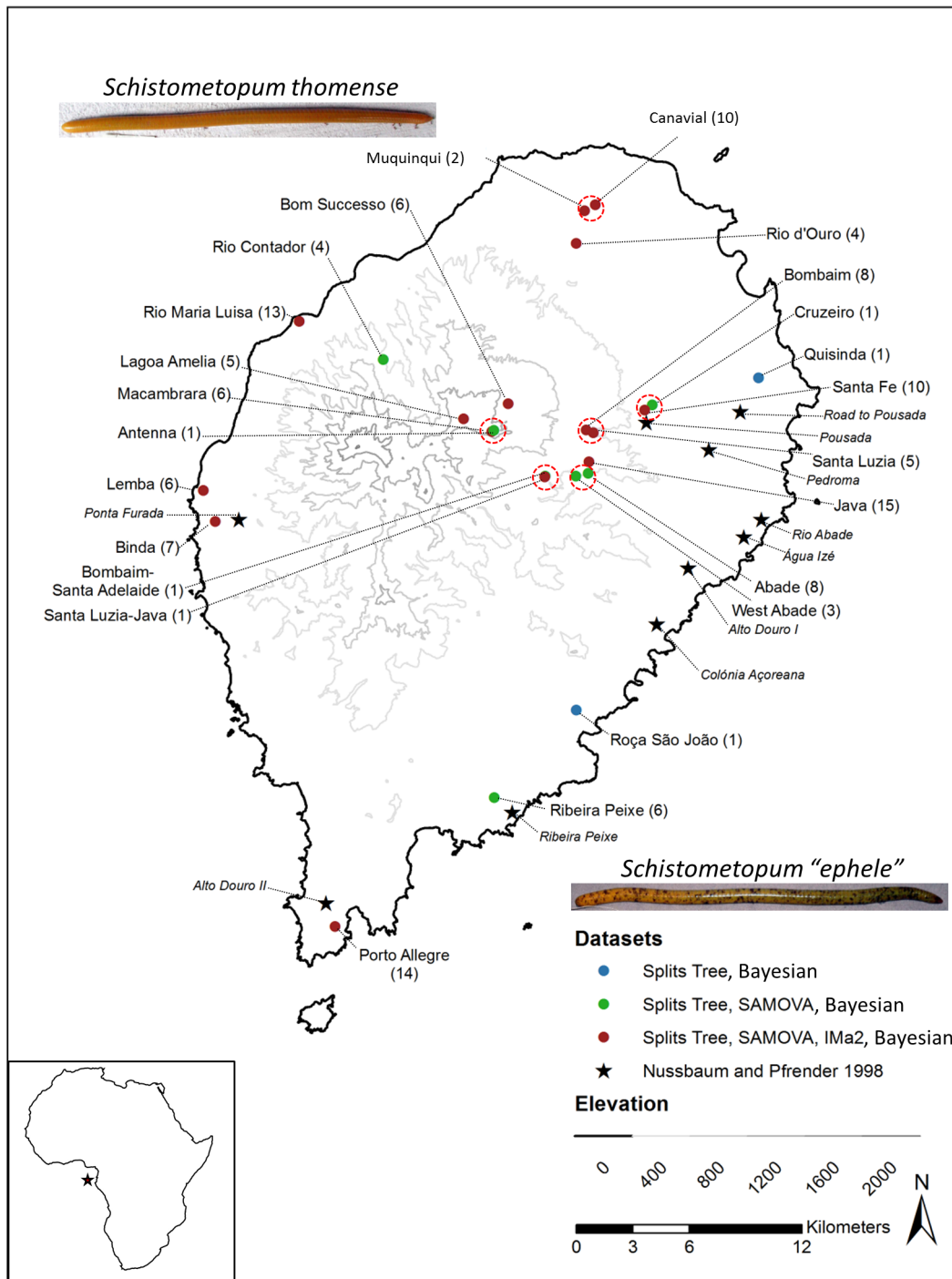


**Figure 1. *Schistometopum thomense* collection localities, São Tomé, Republic of São Tomé and Príncipe.** Numbers in parentheses indicate number of specimens available for genetic analyses. Legend indicates specimens used in Splits Tree, Bayesian, SAMOVA, and/or IMA2 analyses, or discussed by Nussbaum and Pfreder [36] in morphological comparisons. Dashed, red ovals indicate populations lumped for SAMOVA analyses. Photographs show examples of clear and flecked morphs as *Schistometopum thomense* and *Schistometopum "epehele"*, respectively. Red star in lower left panel indicates relative position of São Tomé to continental Africa.  
 doi:10.1371/journal.pone.0104628.g001

for 30 sec., 72°C for 1 min., followed by 72°C for 7 min. Non-hot-start reactions were conducted in 10 µL volumes (1× buffer, 0.175 mM dNTPs, 1.25 mM MgCl<sub>2</sub>, 0.05 U Bioline Taq, 0.54 µM of each primer, 2 µL template DNA) and used the temperature profile: 94°C for 7 min., 25 cycles of 94°C for 30 sec., 50°C for 30 sec.-1 min., 72°C for 1 min., followed by 72°C for

7 min. In addition to ND4, approximately 600 base pairs of the small ribosomal subunit 16S were amplified using the primers 16sar and 16sbr [53] in 10 µL non-hot-start reactions similar to those described above, substituting Apex Taq for Bioline Taq, with the following temperature profile: 94°C for 3 min., 39 cycles

of 94°C for 30 sec., 50°C for 30 sec., 72°C for 1 min., followed by 72°C for 5 min., and dropping to 25°C for 2 minutes.

PCR product was cleaned using the Promega Wizard PCR Preps DNA Purification System (Promega, Madison, WI) following manufacturer's protocol, or with ExoSAP-IT (USB Corporation, Cleveland, OH), using the following reaction conditions: 7.5 µL volumes (0.83 µL 10×SAP Buffer, 0.15 µL SAP Enzyme and 0.08 µL Exo I Enzyme per sample), incubating at 37°C for 15 min., 80°C for 15 min., then cooling to 4°C. Based on visual strength of bands in an agarose gel, 0.5–1.0 µL Wizard Prep product or 1.0–4.5 µL of ExoSAP-IT reaction product were then used in cycle sequencing reactions.

Cycle Sequencing was performed on either a Perkin Elmer 9600, Perkin Elmer 9700 or BioRad thermocycler, following ABI prism instructions for either Big Dye version 2.0 (50 cycles of 96°C for 10 sec, 45°C for 5 sec, and 60°C for 4 min) or Big Dye version 3.1 (either 50 cycles of 96°C for 10 sec, 50°C for 5 sec, and 60°C for 4 min, or 25 cycles of 96°C for 15 sec, 50°C for 15 sec, and 60°C for 4 min) (Perkin-Elmer, Norwalk, CT), depending on which reagent was used. For all samples, amplified products were sequenced in both the 3' and 5' directions, using the original PCR primers. Nucleotide order was read by an ABI-PRISM 3100 Genetic Analyzer (Applied Biosystems, Norwalk, CT). Base calls and editing were resolved by eye using Sequencher versions 3.1 and 4.2 (Gene Codes Corporation, Ann Arbor, MI). Confirmation of ND4 as the amplified product was made with BLAST searches (<http://www.ncbi.nlm.nih.gov/BLAST/>) in GenBank [54].

To confirm that evolutionary patterns in amplified sequences were not obscured by strong selective pressure, standard neutrality tests – Tajima's  $D$  [55–57], Ewens-Watterson homozygosity [58–59], Slatkin's exact test based on Ewens' sampling [60–61], Fu's  $F_s$  [62] and Chakraborty's test of population amalgamation [63] – were run in Arlequin v 3.5 [64].

### Clinal or taxonomic substructure?

We conducted Bayesian phylogenetic analysis in MrBayes version 3.2.0 [65]. The initial model framework for this search was determined with MrModelTest 2.2 [66] using AIC. A 50% majority-rule consensus tree was then generated in MrBayes, using 4 MCMC chains that ran for 120,000 generations, sampling every 10 generations, and using burn-in of 20% via the CIPRES Science Gateway [67]. We assessed stationarity of the model by looking at whether potential scale reduction factor (PSRF) of parameter estimates was close to 1.0 and whether the log probability of the data across MCMC generations was free of any particular pattern.

Geographic substructure was examined in the ND4 dataset using spatial analysis of molecular variance (SAMOVA [68]). This analysis attempts to define the most likely number and composition of geographically-differentiable genetic groups within a dataset by considering the frequency of haplotypes, and the pairwise genetic differences between haplotypes, within and among  $k$  groups relative to that in a total dataset ( $\phi_{CT}$ ). Because SAMOVA performs poorly with datasets populated by low sample-size locations, disjunct sampling localities represented by one individual only were excluded and neighboring and/or remaining low sample size locales ( $n \leq 2$ ) were grouped with proximate larger populations, creating a dataset of 136 individuals from 16 sample sites (SAMOVA sample sites represented in green and blue and lumped populations circled by dashed red lines in Figure 1). Configurations of two through ten possible groupings ( $k$ ) were tested. Best resulting groups were then characterized by amount of haplotype diversity,  $h$  [69], and nucleotide diversity,  $\pi$  [70], and subjected to neutrality tests (Fu's  $F_s$  and Tajima's  $D$ ) to

determine whether any group might be out of mutation drift equilibrium [55–57,62,71]; these tests were run in Arlequin. Fu's  $F_s$  and Tajima's  $D$  tests are sensitive to frequencies of alleles within a sample and will generate significantly negative values when an excess of rare frequency alleles exists, a condition that is expected after recent population expansion. In the instance that a group returned significant values of either of these tests, mismatch distribution analyses were run [72–73] to confirm and to estimate the timing of population expansion. In order to do this, a model of demographic expansion was assumed,  $t = \tau/(2u)$ , in which  $t$  is generation time,  $\tau$  is the age of the expansion in mutational units (estimated in the model of demographic expansion) and  $u$  is the sum of the per nucleotide mutation rate for the region sequenced [72–73]. For *S. thomense*, generation time was set at two years based on reported ages at first reproduction for captive females [41] and  $u$  was estimated from mutation rates of ND4 in amphibians that were available in the literature (the mean of estimates in Arntzen et al. [74] and Wielstra et al. [75]).

To further examine relationships among groups, the full ND4 dataset (138 individuals from 24 populations; sample sites represented by all colored dots in Figure 1) was modeled using a split Neighbor-Net algorithm [76–77] in SplitsTree v 4.11.3 [78]. In addition, uncorrected pairwise genetic distances were calculated using Arlequin. Evidence for isolation-by-distance was explored with Mantel tests [79] in Arlequin, assessing the correlation of Euclidean distances between sample locales with pairwise- $F_{ST}$  values based on uncorrected pairwise distances between haplotypes at those sites; these tests were run for the island sample as a whole and separately for SAMOVA-derived groups that contained  $n > 2$  populations (number of permutations = 16,000).

### Divergence times

To estimate population divergence times, we used SAMOVA-identified population groupings in a coalescent approach, with an Isolation with Migration approach using software IMA2 v 2.0 [80]. The IMA2 software uses a Felsenstein framework to run Markov chain Monte Carlo (MCMC) simulations permitting likelihood-based analyses [81] and allows estimation of time to most recent common ancestor for related phylogenetic groups. We used our Bayesian tree (see above) as a prior input topology for the sampled populations. MCMC parameterization of the model included a burn-in duration of 1,000,000 steps, 10,000 genealogies saved, and geometric heating with 25 chains (0.95 as first and 0.9 as second chain heating parameters). Because preliminary runs showed very different results for populations from the North versus southerly populations, we used a prior file to allow different priors for different populations. Priors were determined by using shorter analysis trials. Three final duplicate runs were submitted to the remote computer cluster running the program IMA2 at Cornell University via internet upload (<http://cbsuapps.tc.cornell.edu/IMA.aspx>). Each run of IMA2 returned a model parameter  $t$  for each lineage pair, as well as the marginal posterior probability densities with 95% upper and lower limits [80]. To estimate divergence time in years ( $T$ ), the geometric mean of the mutation rate ( $U$ ) for the markers sequenced was used:  $T = t/U$  [70–71]. Mutation rates for each marker ( $\mu$ ) per nucleotide site per million years were estimated from amphibian rates for ND4 and 16S in the literature (16S: Vences et al. 2005 [82], ND4: the mean of Arntzen et al. [74] and Wielstra et al. [75]).

### Color

We followed Nussbaum and Pfrender [36] in their scoring of *S. thomense* to one of four different dorsal color classes: 1) light yellow, no brown flecks, 2) dark yellow, no brown flecks, 3) dark

yellow, light to moderate brown flecking, 4) dark yellow, heavy brown flecking. Colors were scored by two of us (RES and GJM) from live animals or from images of animals (after anesthesia). Any disagreements in scores were resolved by reviewing images of specimens concerned.

To test whether color variation was best explained by genetic lineages and/or clinal variation, we treated color coding of ND4-sequenced *S. thomense* ( $n = 138$ ) as a nominal response variable (category 4 serving as the reference) in a multinomial logistic model implemented in PROC GLIMMIX of SAS v 9.2 [83]. (We initially attempted to model color as an ordered response variable, but found that the dataset did not meet the assumptions of ordinal logistic regression.) Explanatory variables were latitude (continuous fixed effect), altitude (continuous fixed effect), geology (categorical fixed effect with four levels: alluvium and flood deposits; basaltic lavas 3–8 Mya; basaltic lavas <1 Mya; and pyroclastic/lava cones <0.4 Mya, based on the underlying geological layer presented in Caldeira et al. [21]), and genetic populations (from SAMOVA results, categorical fixed effect with four levels: Central+East, West, North, and South). We selected these explanatory variables based on previous hypotheses or from proxies when data was unavailable. Specifically, latitude was postulated by Nussbaum and Pfender [36], altitude was found to be important in clinal variation in size [38], geology was selected as a proxy for soil type and vegetation, which are expected to influence caecilian color crypsis [84], and genetic groupings are expected to reveal any taxonomic explanation [34]. Our global model included all main effects described above. To test hypotheses about fixed effects, we ran the global and all nested models, subsequently ranking each model based on AIC<sub>c</sub> scores [85]. We reported the 95% weight candidate model set and examined the support for various covariates by assessing 95% confidence limits around regression parameters.

## Results

### Sequence information

We sequenced approximately 847 base pairs of mitochondrial ND4 DNA (including flanking tRNAs His, Ser, Leu2 [CUN codon]) and 538 additional base pairs of mitochondrial 16S rRNA from 138 and 26 individual *Schistometopum thomense*, respectively, collected at 24 sample locations across the island of São Tomé (Figure 1, Table S1, GenBank accession numbers KM210341-KM210478 [ND4] and KM210479-KM210488, KM210490-KM210506 [16S]; these sequences aligned with positions 10,829–11,675 [5'-3', ND4] and 1,939–2,742 [5'-3', 16S] in the complete mitochondrial genome of *S. thomense* published under GenBank accession GQ244476.1 [86]. Both datasets contained high levels of selectively-neutral heterogeneity: 57 haplotypes and 118 polymorphic nucleotide sites in ND4 and 6 haplotypes and 11 polymorphic nucleotide sites in 16S. These same regions were sequenced in one *Schistometopum gregorii*, collected from Bagamo, Tanzania, (Table S1, GenBank accession numbers KM210507 [ND4] and KM210489 [16S]) for use as an outgroup in phylogenetic analyses.

### Relationships of genetic groups on the island

A Bayesian phylogenetic analysis (model = K80+G) of the ND4 haplotype dataset ( $n_{\text{haplo}} = 57$ ) revealed two deeply divergent and geographically-concordant evolutionary lineages on the island (4.3% minimum uncorrected pairwise genetic distance separating nodes A and B of Bayesian phylogram, Figure 2a). SAMOVA returned five distinct genetic groups, reflecting four geographic lineages – “North” comprising clade A, and “West”, “South” and

“Central+East” representing substructure within clade B – which were clearly distinguished in the Bayesian phylogram as well as in haplotype groupings generated in SplitsTree by Neighbor-Network analyses (Figure 2c). This haplotype network, depicting the relative strength of support for pairwise relationships across all ND4 sequences produced the same four geographically-concordant groupings referenced above, and showed that the deepest divergence lay between the North and all other groups, with North most closely related to the Western group (minimum pairwise genetic distance N vs. W: 4.3%), followed by the two Western off-shoots: the Southern group (N vs. S: 5.3%) and the Central+Eastern group (N vs. C+E: 5.2%) (Figure 2c). The Western group, Central+Eastern group and Southern group were much more closely related to each other than they were to the North ( $\leq 2.0\%$  minimum pairwise genetic distance between all two-way comparisons of these groups). In addition, SAMOVA recognized a fifth group composed of four populations of haplotypes that derived from both the Northern and the Central+Eastern lineages: Macambrara, Java, Abade+West Abade, and Santa Luzia (e.g., “Admixed,” Figure 2a,b). The admixed nature of these four populations was evidenced by bimodal distributions of mismatch analyses (Figure 3), reflecting the paucity of intermediate haplotypes in these “boundary” populations.

In order to provide a more historical interpretation of matrilineal populations, a second SAMOVA was run, for which the four admixed populations were split into their component Northern and Central+Eastern subsets. As expected, this analysis identified the Northern, Western, Central+Eastern, and Southern groups, generating a  $\phi_{CT}$  of 0.892 and explaining nearly 90% of the genetic variation in the island sample. Despite the fact that 79% of haplotypes in our dataset occurred as private alleles – reflected in a very high  $\phi_{ST}$  (0.937) – within population variance explained only 6.34% of the total island variance. Likewise, variance among populations within groups – described by  $\phi_{SC}$ , which was lower (0.412) – explained only 4.45% of total island variance (all  $p$ -values < 0.00001). We found  $\phi_{CT}$  for this SAMOVA continued to rise marginally (<0.01) when the number of possible groups was increased, but adding groups did not significantly change  $\phi_{CT}$  (Figure 4). As illustrated by the  $\phi$ -statistics, genetic variation appeared to be highly substructured on the island. A Mantel test comparing pairwise  $F_{st}$  and Euclidean distance measures across populations within groups found significant evidence of isolation by distance in the Northern group (correlation coefficient = 0.36,  $p = 0.01$ ), but not for the Central+Eastern group.

Within groups, genetic diversity – as measured by haplotype diversity ( $h$ ) and nucleotide diversity ( $\pi$ ) – was highest in the Western and Northern lineages, slightly less variable in the Central+Eastern lineage, and least variable in the Southern lineage (Table 1). The relatively high diversity in the Western lineage was notable, given its low sample size and representation by only two collection locales. The Southern lineage, in contrast, composed of similar sample size but only one locale, had considerably less diversity; each of these groups made up <10% of the total dataset. High observed diversity paired with its relative placement on the Bayesian phylogram indicated that the Western lineage was the first to diverge of the three identified on the southern half of the island (Table 1 and Figure 2a).

IMa2 analysis of a composite ND4 and 16S dataset ( $n_{\text{individuals}} = 26$ , mutation rate 16S: 2.161029, mutation rate ND4: 5.761029) allowed greater insight into lineage ages. Two distinct divergence periods were identified: one between 200–250 Kya and the other between 20–30 Kya. The first divergence between Northern and other lineages produced the highest point for divergence (HPD) at 253 Kya (95% HPD = 136–435 Kya), and the lineage on the west

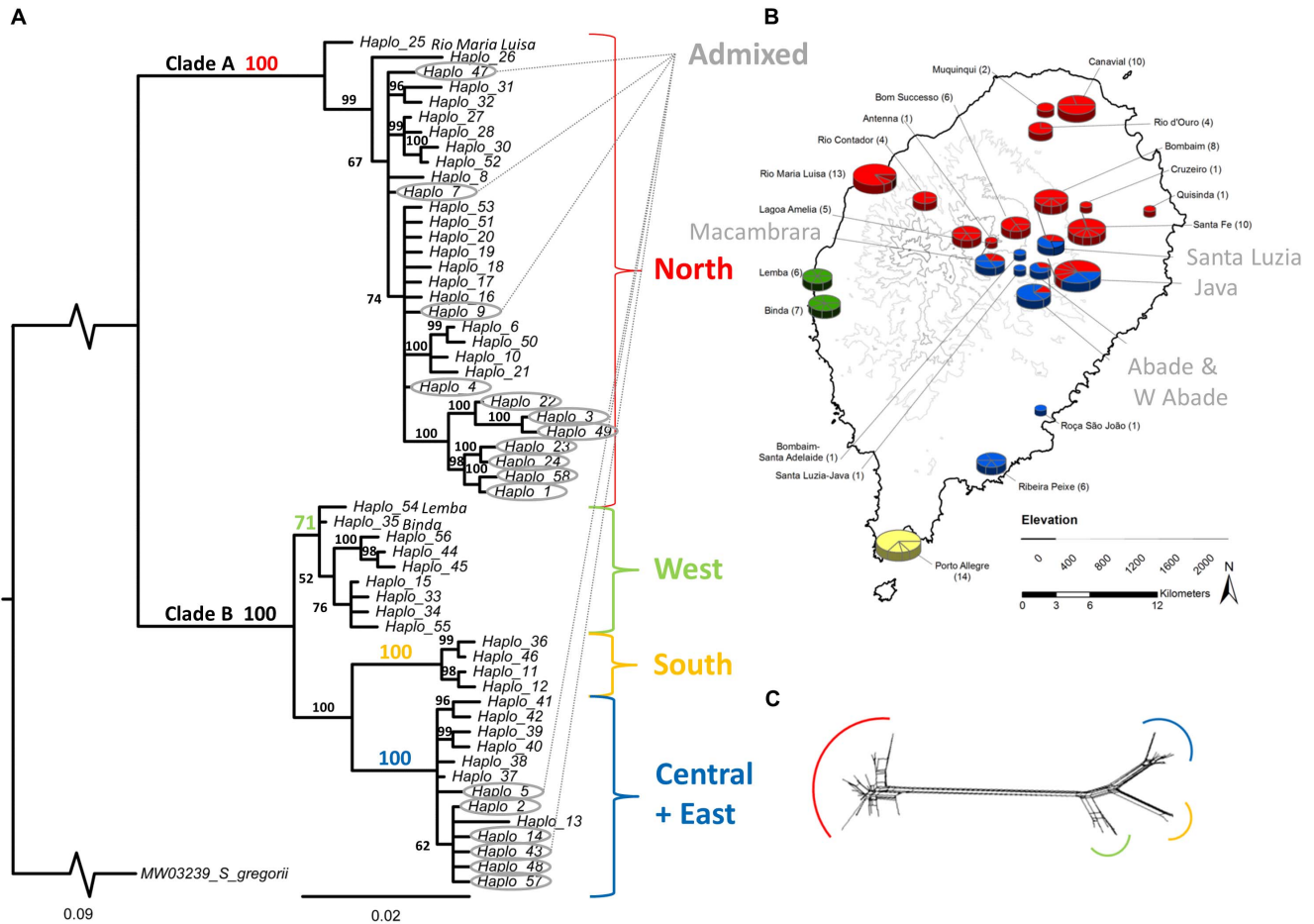


**Figure 2. Genetic and geographic relationships of ND4 haplotypes.** A) Bayesian Phylogram (K80+G, 50% Majority-Rule Consensus Tree), with Bayesian Posterior Probabilities (PP) indicated above branches: Color-coding depicts groups “Admixed”, “North”, “West”, “South” and “Central+East” delineated by SAMOVA analysis. B) Genetic Map by Group displays relative size ( $n_{\text{individuals}}$ ) and haplotype composition of population samples within each group (each pie slice represents one haplotype); bicolored pie charts and gray text indicate admixed populations. C) SplitsTree Neighbor-Net illustrates relative distance between haplotype groups based on uncorrected pairwise genetic distance. Each line represents the connection between two haplotypes with the thicker lines representing many connections. doi:10.1371/journal.pone.0104628.g002

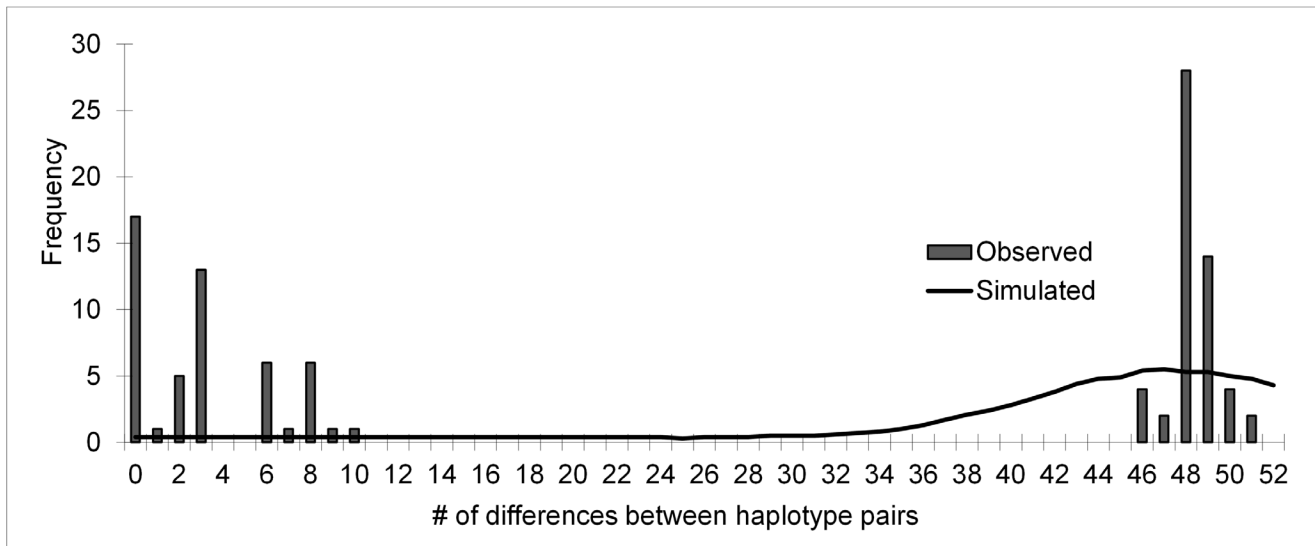


**Figure 3. Mismatch of ND4 haplotypes within population of Java.** Characteristic bimodal distribution of haplotype relationships within admixed populations. doi:10.1371/journal.pone.0104628.g003

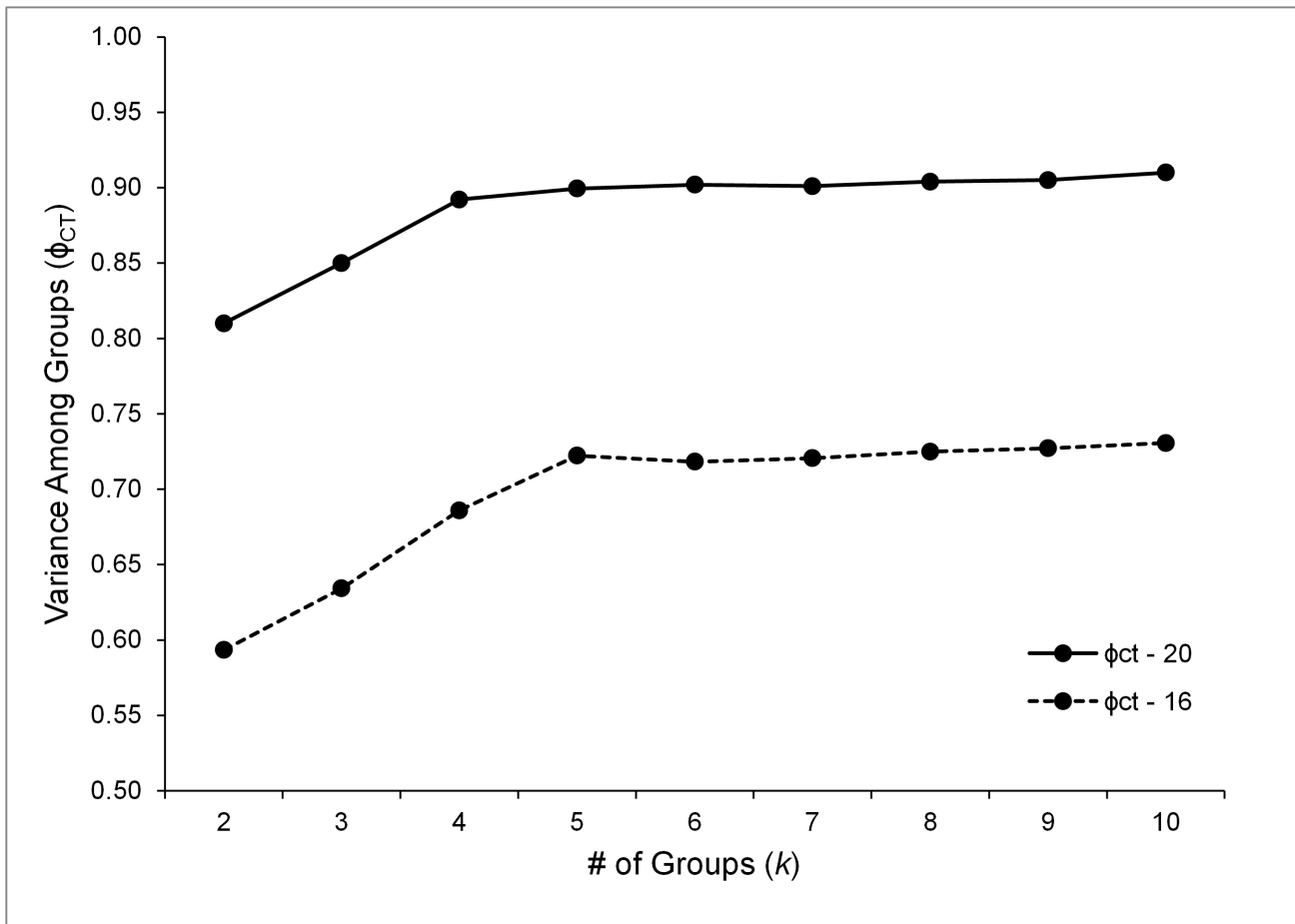


**Figure 4. SAMOVA results illustrating variance in ND4 haplotype diversity attributable to *S. thomense* group structure ( $\phi_{CT}$ ).**  $\phi_{CT} - 16$  illustrates results for initial SAMOVA dataset, in which admixed populations are not split according to haplotype lineage:  $k = 5$  groups explain almost all variation (North, West, Central+East, South, and Admixed).  $\phi_{CT} - 20$  illustrates results for second SAMOVA dataset, in which admixed populations are split according to haplotype lineage:  $k = 4$  groups explain almost all variation (North, West, Central+East, and South). doi:10.1371/journal.pone.0104628.g004

coast appears to have split very close to this time (average HPD = 215 Kya; 95% HPD = 101–354 Kya). Most recently, the lineage in the extreme south diverged from the lineage in the central and eastern areas around 27 Kya (95% HPD = 2–242 Kya). Although 95% HPDs were overlapping for all of these events, the highest point for the HPD for each of the divergence events was used as an indication of the most likely divergence scenario.

Evidence for recent population expansion in the Northern lineage was obtained in results of mismatch analysis, Fu's  $F_s$  and

Tajima's  $D$  (mismatch Sum of Squared Difference = 0.0078,  $p$ -value > 0.5 and Harpending's Raggedness = 0.021,  $p$ -value > 0.3; Fu's  $F_s = -13.08$ ,  $p = 0.0012$ ; Tajima's  $D = -1.80$ ,  $p$ -value = 0.0121), allowing an additional calculation of time since the inferred demographic expansion in the North of São Tomé: ca. 167.5 Kya (based on  $\tau = 2.566$ , 95% CI: 0.182–15.035, which estimated  $t = 83,747$  generations and used a generation time of 2 years). The Central+Eastern and Western groups also showed conformity to a pattern of recent population expansion based on mismatch

**Table 1. Haplotype ( $h$ ) and nucleotide diversity ( $\pi$ )  $\pm$  standard error for four genetic groups of *Schistometopum thomense* identified from 20 sampling sites on the island of São Tomé.**

	North	Central+East	West	South
<i>n</i>	80	31	13	14
<b>ND4 haplotypes</b>	31	13	9	4
<b>Haplotype Diversity (<math>h</math>)</b>	0.93 $\pm$ 0.02	0.84 $\pm$ 0.05	0.95 $\pm$ 0.04	0.58 $\pm$ 0.14
<b>Nucleotide Diversity (<math>\pi</math>)</b>	0.0060 $\pm$ 0.0033	0.0034 $\pm$ 0.0020	0.0042 $\pm$ 0.0026	0.0013 $\pm$ 0.0010

Nucleotide diversity estimates represent the average number of nucleotide differences between two sequences chosen at random [70]. Haplotype diversity estimates represent the likelihood of randomly selecting two different haplotypes from a sample [69].

doi:10.1371/journal.pone.0104628.t001

distribution tests, but for neither of these groups were Tajima's  $D$  or Fu's  $F_s$  significantly negative. The Bayesian phylogram shows the same relative 'ages' of the lineages and the haplotypes within: apparent ancestral haplotypes were collected from the west of the island (Haplotype 25 from Rio Maria Luisa [Northern lineage], and Haplotypes 54 and 15 from Lembra and Binda, respectively [Western lineage], Figure 2a,b).

## Color

Dorsal coloration was mixed within and across all genetic groups, but, on average, animals from the Northern collection localities were lightest and animals from the Central+Eastern collection localities were darkest (Figure 5a, for categories 1 through 4,  $n_1 = 35$ ,  $n_2 = 29$ ,  $n_3 = 33$ ,  $n_4 = 41$ ). Our AIC<sub>c</sub> ordering of multinomial logistic regressions selected the global model – retaining the explanatory variables of genetic group, geology, latitude and altitude – as the best model (AIC<sub>c</sub> = 195.85,  $k = 27$ ), ranking more than 21 AIC<sub>c</sub> units above the next best model and accounting for virtually all the weight among our candidate model set. Despite retaining all explanatory variables, the best model only produced significant Type III effects for genetic group ( $F_{9,111} = 2.3$ ,  $p = 0.02$ ) and latitude ( $F_{3,111} = 3.1$ ,  $p = 0.03$ ). Examination of 95% confidence limits surrounding  $\beta$  estimates indicated that most support for these covariates came from the comparison between dark yellow, unflecked morphs (category 2) to dark yellow, flecked morphs (category 4; Table 2); these unflecked morphs were less likely to have haplotypes in the Central+Eastern group than in the Western group and more likely to have been collected at higher latitudes. They also were less likely to have been collected on basaltic flows <1 Mya than on younger pyroclastic lava cones, and, in general, were less likely to occur in the dataset than the darker, flecked individuals (intercept term “2/4”; Table 2). Latitude similarly affected the relative occurrence of light yellow, unflecked morphs (category 1) to that of the dark yellow, flecked morphs; category 1 morphs were more likely to be found at higher latitudes (Table 2). Overall, given the size of our dataset ( $n = 138$ ) and number of individuals in each response category ( $n_{\text{color}} = \sim 35$ ) relative to total model parameters ( $k = 27$ ), our ability to detect significant effects may have been restricted. For the geology covariate, sample size may have limited the power to detect an effect in some levels, e.g., only one specimen resided on older basaltic lava flows 3–8 Mya (Figure 6). Further observations from raw data showed that within populations of  $n \geq 2$ , substantial variation existed; more than 25% of the populations contained both clear and flecked individuals (Figure 5b). Of the seven collection locales that contained clear and flecked individuals, only one was genetically admixed (Macambrara); the remainder were uniquely Northern, Western, or Southern. We expect that investigation of nDNA patterns in these and the other admixed populations will clarify questions that remain about the interplay of color morphology and genotype for these caecilians.

## Discussion

Our results suggest that both genetic clades and clinal variation contribute to the strikingly high differences in coloration that led Taylor [34] to describe *Schistometopum “ephelē”* as a distinct taxon from *Schistometopum thomense* on the island of São Tomé. Nussbaum and Pfrender [36] showed the importance of increased sampling in their work aimed at unraveling historic discrepancies in *Schistometopum* taxonomy. In contrast to their results, which identified a morphological cline only, our wider sampling (especially in the North), coupled with genetic data, show that *S.*

*thomense*, as currently recognized, is highly structured for mtDNA and that this structure is concordant with northern, western, eastern+central and southern geographic groupings on the island. Although, a north-south cline is not rejected by our morphological analyses (i.e., inclusion of the latitude covariate in our best multinomial logistic regression), our mitochondrial genetic results show that this species exhibits a narrow zone of admixture between the two most divergent clades (~4% minimum uncorrected pairwise distance between ND4 lineages) and ages this split at approximately 0.25 Mya. We require nDNA sequencing to ascertain whether the admixed area contains hybrids between the two mtDNA lineages. However, the mixed nature of color forms in these areas suggests that this is the case. Admixed zones have been found for other amphibians which have arrived on islands [87], and for natural populations in a ring species [88], and this challenges the traditional view of genetic equilibrium in population genetics. In our example from the island of São Tomé, we suggest that environmental disturbance (volcanism) is capable of producing these highly structured groupings.

Whether *S. thomense* arrived on São Tomé by a single or multiple colonization events remains inconclusive, given the relatively recent estimates of population divergence (relative to island age) and of volcanic flows. Multiple independent colonization events have been suggested for geckos [22–23], skinks [24] and various snake species [25]. Despite an approximate (sub-aerial) age of 13 Mya for the island [18], two of these studies have produced remarkably recent dates for colonizations and radiations on the island: ca 800 Kya and ca 200 Kya for skinks [24], and ca 800 Kya and ca 600 Kya for passerine birds (*Zosterops* spp. and *Speirops* spp., respectively) [89]. As pointed out by Jesus et al. [24], volcanic activity may be responsible for these recent dates, either having wiped out evidence of earlier colonizations or having provided impetus for diversification.

The most recent eruptions have been placed at 36 Kya, in geologic samples collected from the islet of Rolas (immediately South of our most southerly collection locale, Porto Alegre on São Tomé) [19]. This date is close to our most recent estimated date for population divergence which also corresponds to the split between the southern population, and the eastern population (of which the next nearest sampling locale was Ribeira Peixe, approximately 11 km northeast). We infer this corroboration in dates defining population groups as an indication that volcanism on São Tomé is the likely cause of other genetic groups that we define. The northern population group corresponds well with the <1Ma northern lava flow (Figure 5). The geological map shows that the North of the island contains numerous small pockets along the coast which could have acted as refugia. This scenario also corresponds with the estimated date of expansion of this northern population. Interestingly, the admixed populations occur almost exactly on the borders of this area suggesting recolonization from southern populations was limited although the reason for this is unclear. Although we cannot rule out that genetic groups may represent separate colonization events, especially in light of an apparently ideal delivery system [27], we speculate that volcanic activity is capable of producing these genetic patterns. Alternatively, our results could be explained by a combination of volcanic activity (Central+East, West and South) and multiple colonization events (North and all others: Central+East, West and South); i.e., both taxonomic and clinal variation. Sampling of the elusive taxon from the Democratic Republic of the Congo may prove critical in eliminating this hypothesis.

Amphibians have been classically described as highly philopatric [90], with strong population structuring over relatively small spatial scales [91–92]. Caecilians, in particular, have been

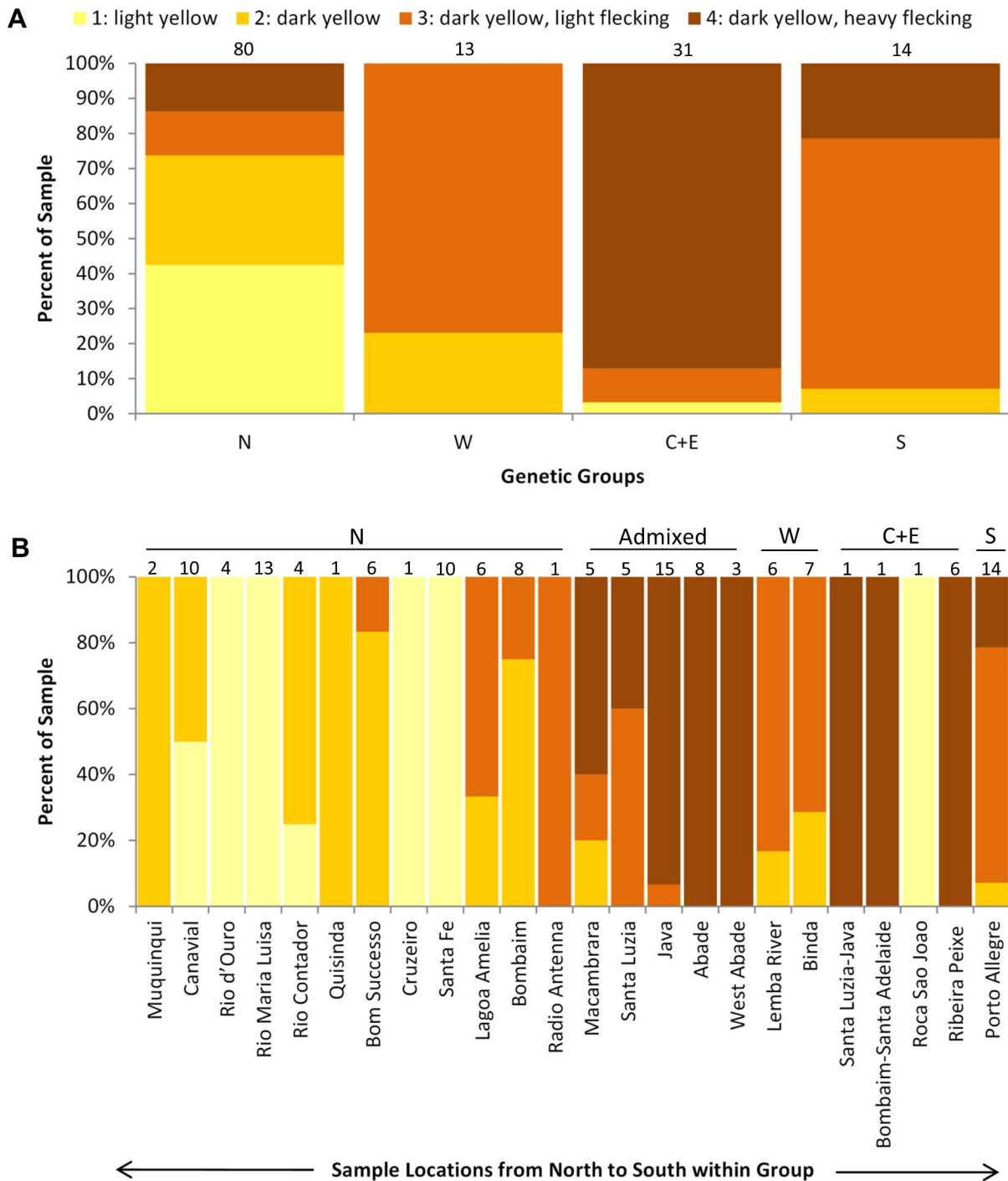


**Figure 5. Color categorization of specimens based on Nussbaum and Pfrender's [36] ventral color descriptions. A) By haplotype group, and B) By collection locality.** Numbers above bars are sample sizes ( $n_{total} = 138$ ). N = North, C+E = Central+East, W = West, S = South, and Admixed = admixed populations containing haplotypes in both the Northern and Central+Eastern genetic groups. doi:10.1371/journal.pone.0104628.g005

considered poor dispersers because of their fossorial nature and sensitivity to the moisture content of surrounding environments [93–94]. However, the only published study of intraspecific caecilian genetics (*Ichthyophis* sp. from the Western Ghats of India) suggests that caecilians are not necessarily philopatric [95], although a more recent study from Southeast Asia suggests much

higher structuring over a far smaller area [96]. The strong population genetic structure shown in our study, together with the large number of private alleles, is therefore more in line with this and the traditional view of amphibians, and is somewhat extreme given the small size of the island and almost ubiquitous occupancy of this species on São Tomé (RCD, GJM & RES *pers. obs.*). An

**Table 2.** Regression coefficients (odds ratios) and 95% confidence limits from top AIC<sub>c</sub>-ranked model returned by multinomial logistic regression of dorsal color on genetic group, latitude, altitude and geology.

	model coefficients (odds ratios)	$\beta$ estimate	95% CL
<b>intercepts</b>	1/4	-31.89	-68.79, 5.01
	2/4	-32.95*	-64.97, -0.93
	3/4	-17.16	-49.73, 15.42
	alluvial/cone (1/4)	9.89	-51.82, 71.59
	alluvial/cone (2/4)	12.49	-48.57, 73.64
	alluvial/cone (3/4)	11.99	-48.53, 72.50
<b>geology</b>	basalt 3–8 Mya/cone (1/4)	21.87	-34.46, 78.31
	basalt 3–8 Mya/cone (2/4)	27.19	-87.37, 141.75
	basalt 3–8 Mya/cone (3/4)	15.42	-78.32, 109.16
	basalt <1 Mya/cone (1/4)	2.61	-4.90, 10.11
	basalt <1 Mya/cone (2/4)	-3.84*	-7.45, -0.23
	basalt <1 Mya/cone (3/4)	-3.50	-7.07, 0.07
<b>latitude</b>	1/4	126.07*	11.21, 240.94
	2/4	175.41*	60.69, 290.14
	3/4	113.22	-2.11, 228.55
<b>altitude</b>	1/4	-0.03	-0.05, 0.00
	2/4	0.00	-0.00, 0.01
	3/4	0.00	-0.00, 0.01
	C+E/W (1/4)	1.94	-25.32, 29.21
	C+E/W (2/4)	-20.89*	-40.73, -1.05
	C+E/W (3/4)	-15.52	-32.52, 1.48
<b>genetic group</b>	N/W (1/4)	6.21	-19.69, 32.10
	N/W (2/4)	-14.24	-31.32, 2.85
	N/W (3/4)	-13.37	-30.18, 3.45
	S/W (1/4)	22.77	-14.53, 60.07
	S/W (2/4)	25.10	-3.42, 53.62
	S/W (3/4)	13.97	-15.03, 42.96

Odds ratios are interpreted as the likelihood of being in a particular category in reference to a baseline (e.g., for the model coefficient “geology: alluvial/cone (1/4),” the  $\beta$  estimate represents the probability of being in color category 1 versus 4 given that animal was collected on alluvial soil versus a lava cone). Significant  $\beta$  estimates are indicated by an asterisk.

doi:10.1371/journal.pone.0104628.t002

explanation for these two very different results for caecilian taxa may stem from the Indian study being based on a very small sample ( $n = 18$ ) using relatively undifferentiated mtDNA markers (12S and 16S) in a phylogeographic context [95]. Our study is therefore, the first population genetic study of any caecilian and we suggest that our results showing strong genetic structuring over very small spatial scales may be represented more widely by many terrestrial gymnophiones. Our results have important implications for conservation of caecilians, especially where populations have become fragmented.

We emphasize provisional acceptance of our results given potential bias posed by use of a two-gene mtDNA dataset. Because (1) natural selection influences mutations in functional genes, (2) the coalescence of gene lineages to cladogenic events may be slow to reflect organismal phylogeny or gene lineages may diverge within a taxonomic line and insinuate a taxonomic division when one does not exist, and (3) – for most taxa – mitochondrial phylogenies track only the evolutionary history of matriarchal lines, we highlight the fact that cladogenic results reported here require substantiation with nDNA. However, we note that single-gene mtDNA histories have proven informative in many studies

[97–105] and that our dataset appears to be an appropriate information source for *S. thomense* on São Tomé given the neutral behavior of the mutations observed, the geographic congruence of haplotype pattern, and the generalized concordance with morphological data.

## Conclusions

*Schistometopum thomense* on São Tomé has a strongly differentiated population structure shown by mtDNA, something that was hitherto unknown for any species in this amphibian Order. Our study confirms previous hypotheses concerning clinal latitudinal variation [36] and philopatry [38], but was inconclusive about the importance of color for crypsis [84] using our geological proxy for soil type and vegetation type. Taxonomically, our results were inconclusive because we could not investigate a clear zone of admixture present on the island between two deeply divergent clades (which would correspond to *S. thomense* and *S. ephèle*), although applying genetic barcoding standards to 16S [82,106], our 4.3% divergence would not be considered deep enough to warrant taxonomic differentiation. Further investigation into the

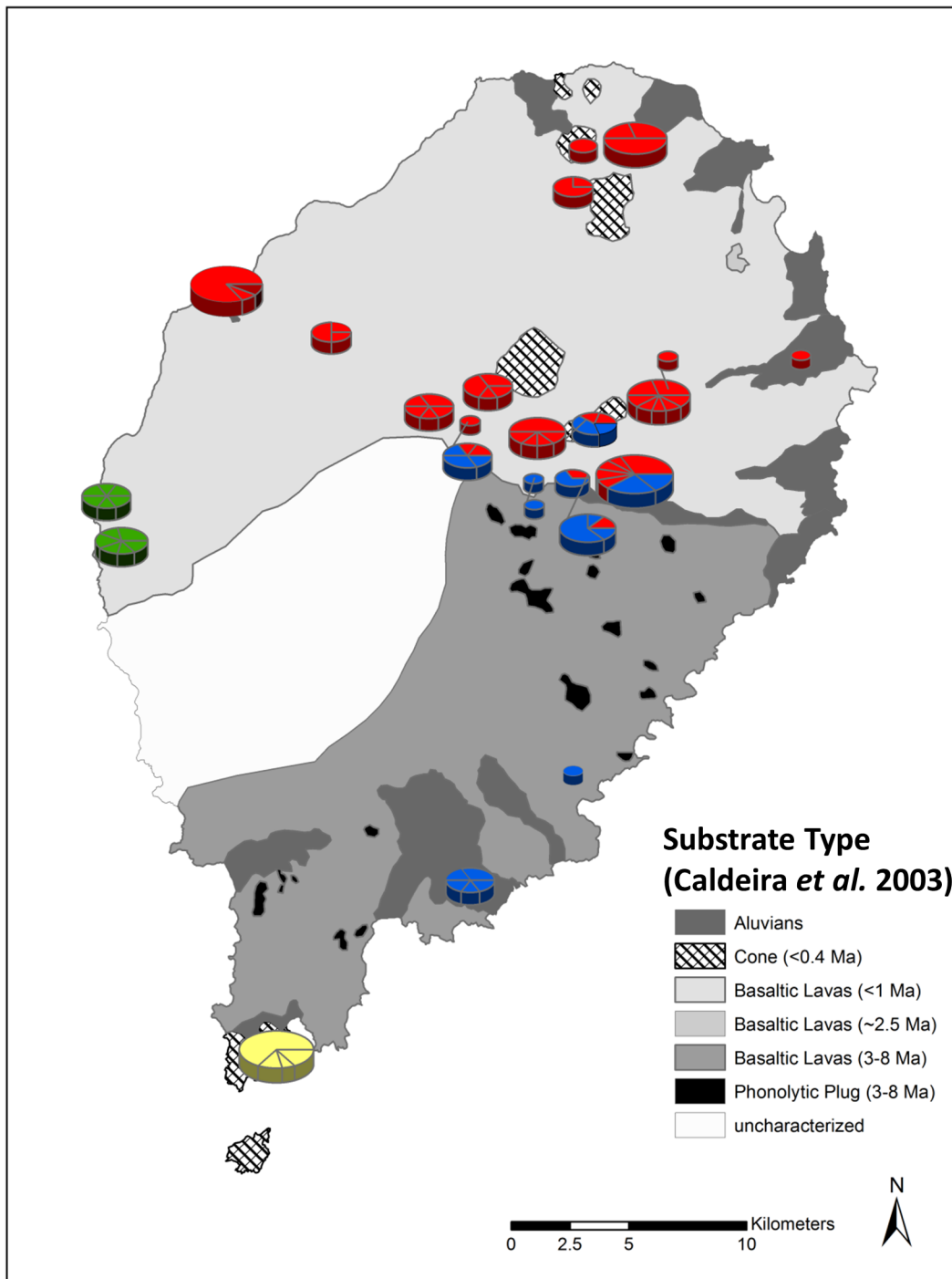


**Figure 6. Distribution of haplotype groups in relation to island volcanism.** Geologic data borrowed from Figure 1 of Caldeira *et al.* [21]. doi:10.1371/journal.pone.0104628.g006

admixed zone is required with nDNA to provide more conclusive genetic results.

### Supporting Information

**Abstract S1** Resumo. Abstract in Portuguese. (DOCX)

**Table S1** Specimen Data. (DOCX)

### Acknowledgments

We would like to acknowledge the assistance and contributions of the following people, instrumental at various stages of this work: Jens Vindum, Dr. Marc Delêtre, Dr. Josef Uyeda, Dr. Tomio Iwamoto, Angus Gascoigne, Ned Seligman and Quintino Quade as well as other field assistants (for collection of specimens); Drs. Mark Wilkinson and Simon Loader (for provision of outgroup tissue); Boni Cruz, Kristy Deiner, and Anna Sellas (for laboratory guidance and access to phylogenetic software); Michelle Koo (for initial GIS mapping); and Drs. Jack Dumbacher, Peter

Roopnarine and Eric Routman (for assistance with earlier-stage coding and analyses in PAUP, MrBayes and Arlequin). Comments from three reviewers greatly helped in our revision of this manuscript.

## References

- Darwin C (1859) On the origin of species by means of natural selection, or the preservation of favoured races in the struggle for life, 1<sup>st</sup> ed. London: John Murray. 502 p.
- MacArthur RH, Wilson EO (1963) An equilibrium theory of insular zoogeography. *Evolution* 17: 373–387.
- MacArthur RH, Wilson EO (1967) The theory of island biogeography. Princeton: Princeton University Press. 205 p.
- Losos JB, Schluter D (2000) Analysis of an evolutionary species-area relationship. *Nature* 408: 847–850.
- Ricklefs RE, Lovette IJ (1999) The role of island area *per se* and habitat diversity in the species-area relationships of four Lesser Antillean faunal groups. *J Anim Ecol* 68: 1142–1160.
- Filardi CE, Moyle RG (2005) Single origin of a pan-Pacific bird group and upstream colonization of Australasia. *Nature* 438: 216–219.
- Whittaker RJ, Triantis KA, Ladle RJ (2008) A general dynamic theory of oceanic island biogeography. *J Biogeogr* 35: 977–994.
- Losos JB, Ricklefs RE (2009) Adaptation and diversification on islands. *Nature* 457: 830–836.
- Kier G, Krefl H, Lee TM, Jetz W, Ibsch PL, et al. (2009) A global assessment of endemism and species richness across island and mainland regions. *Proc Natl Acad Sci U S A* 106: 9322–9327.
- Losos JB, Jackman TR, Larson A, de Queiroz K, Rodriguez-Schettino R (1998) Historical contingency and determinism in replicated adaptive radiations of island lizards. *Science* 279: 2115–2118.
- de Queiroz A (2014) The monkey's voyage: how improbable journeys shaped the history of life. New York: Basic Books. 360 p.
- Vences M, Freyhof J, Sonnenberg R, Kosuch J, Veith M (2001) Reconciling fossils and molecules: Cenozoic divergence of cichlid fishes and the biogeography of Madagascar. *J Biogeogr* 28: 1091–1099.
- Vicario S, Caccone A, Gauthier J (2003) Xantusiid “night” lizards: a puzzling phylogenetic problem revisited using likelihood-based Bayesian methods on mtDNA sequences. *Mol Phylogenet Evol* 26: 243–261.
- Trewick SA (2000) Molecular evidence for dispersal rather than vicariance as the origin of flightless insect species on the Chatham Islands, New Zealand. *J Biogeogr* 27: 1189–1200.
- Figueiredo E, Paiva J, Stévant T, Oliveira F, Smith GF (2011) Annotated catalogue of the flowering plants of São Tomé and Príncipe. *Bothalia* 41: 41–82.
- Mendes LF, de Sousa B (2012) New account of the butterflies (Lepidoptera: Rhopalocera) of São Tomé e Príncipe. *Boletín de la Sociedad Entomológica Aragonesa* 51: 157–186.
- Melo M (2006) Bird speciation in the Gulf of Guinea. PhD thesis. Edinburgh: University of Edinburgh.
- Lee D-C, Halliday AN, Fitton JG, Poli G (1994) Isotopic variations with distance and time in the volcanic islands of the Cameroon line: evidence for a mantle plume origin. *Earth Planet Sci Lett* 123: 119–138.
- Barfod DN, Fitton JG (2012) Pleistocene volcanism on São Tomé, Gulf of Guinea, West Africa. *Quat Geochronol* 21: 77–89. Available: <http://dx.doi.org/10.1016/j.quageo.2012.11.006>. Accessed 11 Apr 2013.
- Caldeira R, Munhá JM (2002) Petrology of ultramafic nodules from São Tomé Island, Cameroon Volcanic Line (oceanic sector). *J Afr Earth Sci* 34: 231–246.
- Caldeira R, Madeira J, Munhá JM, Afonso R, Mata J, et al. (2003) Caracterização das principais unidades vulcano-estratigráficas da ilha de S. Tomé, Golfo da Guiné. *Ciências da Terra (UNL)*, Lisboa, no. esp. V, CD-ROM: A15–A18.
- Jesus J, Brehm A, Harris D (2005a) Phylogenetic relationships of *Hemidactylus* geckos from the Gulf of Guinea islands: patterns of natural colonizations and anthropogenic introductions estimated from mitochondrial and nuclear DNA sequences. *Mol Phylogenet Evol* 34: 480–485.
- Miller EC, Sellas AB, Drewes RC (2012) A new species of *Hemidactylus* (Squamata: Gekkonidae) from Príncipe Island, Gulf of Guinea, West Africa with comments on the African-Atlantic clade of *Hemidactylus* geckos. *Afr J Herpetol* 61: 40–57.
- Jesus J, Brehm A, Harris D (2005b) Phylogeography of *Mabuya maculilabris* (Reptilia) from São Tomé Island (Gulf of Guinea) inferred from mtDNA sequences. *Mol Phylogenet Evol* 37: 503–510.
- Jesus J, Nagy ZT, Branch WR, Wink M, Brehm A, et al. (2009) Phylogenetic relationships of African green snakes (genera *Philothamnus* and *Hapsidophrys*) from São Tomé, Príncipe and Annobon islands based on mtDNA sequences, and comments on their colonization and taxonomy. *Herpetol J* 19: 41–48.
- Vences M, Vieites DR, Glaw F, Brinkmann H, Kosuch J, et al. (2003) Multiple overseas dispersal in amphibians. *Proc Biol Sci* 270: 2435–2442.
- Measey GJ, Vences M, Drewes RC, Chiari Y, Melo M, et al. (2007) Freshwater paths across the ocean: molecular phylogeny of the frog *Ptychadena newtoni* gives insights into amphibian colonization of oceanic islands. *J Biogeogr* 34: 7–20.
- Townsend TM, Tolley KA, Glaw F, Böhme W, Vences M (2010) Eastward from Africa: palaeocurrent-mediated chameleon dispersal to the Seychelles Islands. *Biol Lett* 7: 225–228.
- Samonds KE, Godfrey LR, Ali JR, Goodman SM, Vences M, et al. (2012) Spatial and temporal arrival patterns of Madagascar's vertebrate fauna explained by distance, ocean currents, and ancestor type. *Proc Natl Acad Sci U S A* 109: 5352–5357.
- de Queiroz A (2005) The resurrection of oceanic dispersal in historical biogeography. *Trends Ecol Evol* 20: 68–73.
- Gower D, Wilkinson M (2005) Conservation biology of caecilian amphibians. *Conserv Biol* 19: 45–55.
- Barboza du Bocage JV (1873) *Mélanges Erpétologiques*. *Jornal de Sciéncias Mathematicas Physicas e Naturas*, Lisboa 4: 209–232.
- Loader SP, Pisani D, Cotton JA, Gower DJ, Day JJ, et al. (2007) Relative time scales reveal multiple origins of parallel disjunct distributions of African caecilian amphibians. *Biol Letters* 3(5): 505–508.
- Taylor ED (1965) New Asiatic and African caecilians with redescrptions of certain other species. *Sci Pap Univ Kansas Nat Hist Mus* 46: 253–302.
- Peters W (1874) Über neue Amphibien (*Gymnopsis*, *Siphonops*, *Polypedates*, *Rhacophorus*, *Hyla*, *Cyclodus*, *Euprepes*, *Clemmys*). *Monatsbericht Königl. Akademie Wissenschaften Berlin* 1874: 616–625 + 2 plates.
- Nussbaum RA, Pfrender ME (1998) Revision of the African caecilian genus *Schistometopum* Parker (Amphibia: Gymnophiona: Caeciliidae). *Misc Publ Mus Zool Univ Mich* 187. iv+32 p.
- Peters W (1880) Über neue oder weniger bekannte Amphibien des Berliner Zoologischen Museums (*Leposoma dispar*, *Monopeltis* (*Phractogonus*) *jugalensis*, *Typhlops depressus*, *Leptocalamus trilineatus*, *Xenodon punctatus*, *Elapomorphus erythronotus*, *Hylomantis fallax*). *Monatsbericht Königl. Akademie Wissenschaften Berlin* 1880: 217–224 + 1 plate.
- Measey GJ, Van Dongen S (2006) Bergmann's rule and the terrestrial caecilian *Schistometopum thomense* (Amphibia: Gymnophiona: Caeciliidae). *Evol Ecol Res* 8: 1049–1059.
- Seyahooei MA, van Alphen JJM, Kraaijeveld K (2011) Genetic structure of *Leptopilina bouardi* populations from different climatic zones of Iran. *BMC Ecol* 11: 1–9.
- Wilkinson M, San Mauro D, Sherratt E, Gower DJ (2011) A nine-family classification of caecilians (Amphibia: Gymnophiona). *Zootaxa* 2874: 41–64.
- Haft J, Franzen M (1996) Freilandbeobachtungen, Verhalten und Nachzucht der São Tomé-Blindwühle *Schistometopum thomense* (Bocage, 1873). *Herpetofauna* 18: 5–11.
- Haft J (1992) Bemerkungen zu den Blindwühlen der Gattung *Schistometopum* von São Tomé (Gymnophiona, Caeciliidae). *Bonn Zool Beitr* 43: 477–479.
- Loumont C (1992) Les Amphibiens de São Tomé et Príncipe: révision systématique, cris nuptiaux et caryotypes. *Alytes* 10: 37–62.
- Schätti B, Loumont C (1992) Ein Beitrag zur Herpetofauna von São Tomé (Golf von Guinea) (Amphibia et Reptilia). *Zool Abh* 47: 23–36.
- Fahr J (1993) Ein Beitrag zur Biologie der Amphibien der Insel São Tomé (Golf von Guinea) (Amphibia). *Zool Abh* 19: 75–84.
- Delêtre M, Measey GJ (2004) Sexual selection vs. ecological causation in a sexually dimorphic caecilian *Schistometopum thomense* (Amphibia: Gymnophiona: Caeciliidae). *Ethology, Ecology and Evolution* 16: 243–253.
- Stoelting RE (2006) Microevolutionary implications of genetic variation in the São Tomé Caecilian, *Schistometopum thomense* (Gymnophiona: Caeciliidae). Master's thesis. San Francisco: San Francisco State University.
- Measey GJ (2006) Surveying biodiversity of soil herpetofauna: towards a standard quantitative methodology. *Eur J Soil Biol* 42(Suppl): 103–110.
- Dallimer M, King T, Atkinson RJ (2009) Pervasive threats within a protected area: conserving the endemic birds of São Tomé, West Africa. *Anim Conserv* 12: 209–219.
- Measey J, Drewes R, Wilkinson M, Loader S (2004) *Schistometopum thomense*. In: IUCN Red List of Threatened Species v 2010.1. Available: <http://www.iucnredlist.org>. Accessed 18 Jul 2010.
- Burbrink FT, Lawson R, Slowinski JB (2004) Mitochondrial DNA phylogeny of the polytypic North American rat snake (*Elaphe obsoleta*): a critique of the subspecies concept. *Evolution* 54: 2107–2118.
- Arévalo E, Davis SK, Sites Jr JW (1994) Mitochondrial DNA sequence divergence and phylogenetic relationships among eight chromosome races of the *Sceloporus grammicus* complex (Phrynosomatidae) in central Mexico. *Syst Biol* 43: 387–418.
- Palumbi SR (1996) *Nucleic Acids II: The polymerase chain reaction*. In: Hillis DM, Moritz C, Mable BK, editors. *Molecular Systematics*. Sunderland: Sinauer Assoc Inc. pp. 205–247.
- Benson AB, Karsh-Mizrachi I, Lipman DJ, Ostell J, Wheeler DL (2004) GenBank: update. *Nucleic Acids Res* 32: D23–D26.

## Author Contributions

Conceived and designed the experiments: RES GJM. Performed the experiments: RES GJM. Analyzed the data: RES GJM. Contributed reagents/materials/analysis tools: RES GJM RCD. Wrote the paper: RES GJM RCD.

55. Tajima F (1989a) Statistical method for testing the neutral mutation hypothesis by DNA polymorphism. *Genetics* 123: 585–595.
56. Tajima F (1989b) The effect of change in population size on DNA polymorphism. *Genetics* 123: 597–601.
57. Tajima F (1993) Measurement of DNA polymorphism. In: Takahata N, Clark AG, editors. *Mechanisms of molecular evolution: introduction to molecular paleopopulation biology*. Sunderland: Sinauer Associates, Inc. pp. 37–59.
58. Watterson G (1978) The homozygosity test of neutrality. *Genetics* 88: 405–417.
59. Watterson G (1986) The homozygosity test after a change in population size. *Genetics* 112: 899–907.
60. Slatkin M (1994) An exact test for neutrality based on the Ewens sampling distribution. *Genet Res* 64: 71–74.
61. Slatkin M (1996) A correction to the exact test based on the Ewens sampling distribution. *Genet Res* 68: 259–260.
62. Fu Y-X (1997) Statistical tests of neutrality of mutations against population growth, hitchhiking and background selection. *Genetics* 147: 915–925.
63. Chakraborty R (1990) Mitochondrial DNA polymorphism reveals hidden heterogeneity within some Asian populations. *Am J Hum Genet* 47: 87–94.
64. Excoffier L, Lischer HEL (2010) Arlequin suite ver 3.5: a new series of programs to perform population genetics analyses under Linux and Windows. *Mol Ecol Resour* 10: 564–567.
65. Ronquist F, Teslenko M, van der Mark P, Ayres D, Darling A, et al. (2012) MrBayes 3.2: Efficient Bayesian phylogenetic inference and model choice across a large model space. *Syst Biol* 61: 539–542.
66. Nylander JAA (2004) MrModeltest v 2. Program distributed by the author. Evolutionary Biology Centre, Uppsala University.
67. Miller MA, Pfeiffer W, Schwartz T (2010) Creating the CIPRES Science Gateway for inference of large phylogenetic trees. In: *Proceedings of the Gateway Computing Environments Workshop (GCE)*, 14 Nov. 2010, New Orleans, LA. pp. 1–8.
68. Dupanloup I, Schneider S, Excoffier L (2002) A simulated annealing approach to define the genetic structure of populations. *Mol Ecol* 11: 2571–2581.
69. Nei M (1987) *Molecular Evolutionary Genetics*. New York: Columbia University Press. p. 180.
70. Nei M, Li W-H (1979) Mathematical model for studying genetic variation in terms of restriction endonucleases. *Proc Natl Acad Sci USA* 76: 5269–5273.
71. Schneider S, Excoffier L (1999) Estimation of demographic parameters from the distribution of pairwise differences when the mutation rates vary among sites: Application to human mitochondrial DNA. *Genetics* 152: 1079–1089.
72. Rogers A (1995) Genetic evidence for a Pleistocene population explosion. *Evolution* 49: 608–615.
73. Rogers AR, Harpending H (1992) Population growth makes waves in the distribution of pairwise genetic differences. *Mol Biol Evol* 9: 552–569.
74. Arntzen JW, Espregueira Themudo G, Wielstra B (2007) The phylogeny of crested newts (*Triturus cristatus* superspecies): nuclear and mitochondrial genetic characters suggest a hard polytomy, in line with the paleogeography of the centre of origin. *Contrib Zool* 76: 4. Available: <http://dpc.uba.uva.nl/ctz/vol76/nr04/art05>. Accessed 2012.
75. Wielstra B, Themudo GE, Güçlü O, Olgun K, Poyarkov NA, et al. (2010) Cryptic crested newt diversity at the Eurasian transition: the mitochondrial DNA phylogeography of Near Eastern *Triturus* newts. *Mol Phylogenet Evol* 56: 888–896.
76. Bryant D, Moulton V (2004) Neighbor-net: an agglomerative method for the construction of phylogenetic networks. *Mol Biol Evol* 21: 255–265.
77. Huson DH, Scornavacca C (2011) A survey of combinatorial methods for phylogenetic networks. *Genome Biol Evol* 3: 23–35.
78. Huson DH, Bryant D (2006) Application of Phylogenetic Networks in Evolutionary Studies. *Mol Biol Evol* 23: 254–267.
79. Mantel N (1967) The detection of disease clustering and a generalized regression approach. *Cancer Res* 27: 209–220.
80. Hey J (2010) Isolation with migration models for more than two populations. *Mol Biol Evol* 27: 905–920.
81. Hey J, Nielsen R (2007) Integration within the Felsenstein equation for improved Markov chain Monte Carlo methods in population genetics. *Proc Natl Acad Sci U S A* 104: 2785–2790.
82. Vences M, Thomas M, Bonnett RM, Vieites DR (2005) Deciphering amphibian diversity through DNA barcoding: chances and challenges. *Philos T Roy Soc B* 360: 1859–1868.
83. Littell RC, Milliken GA, Stroup WW, Wolfinger RD, Schnabenberger O (2006) SAS for Mixed Models. Cary, NC: SAS Institute Inc. 814 p.
84. Wollenberg KC, Measey GJ (2009) Why colour in subterranean vertebrates? Exploring the evolution of colour patterns in caecilian amphibians. *J Evol Biol* 22: 1046–1056.
85. Burnham KP, Anderson DR (2002) *Model Selection and Multimodel Inference: A Practical Information-Theoretic Approach*. New York: Springer-Verlag. 488 p.
86. Zhang P, Wake MH (2009) A mitogenomic perspective on the phylogeny and biogeography of living caecilians (Amphibia: Gymnophiona). *Mol Phylogenet Evol* 53: 479–491.
87. Estoup A, Wilson IJ, Sullivan C, Cornuet JM, Moritz C (2001) Inferring population history from microsatellite and enzyme data in serially introduced cane toads, *Bufo marinus*. *Genetics* 159: 1671–1687.
88. Moritz C, Schneider CJ, Wake DB (1992) Evolutionary relationships within the *Ensatina eschscholtzii* complex confirm the ring species interpretation. *Syst Biol* 41: 273–291.
89. Melo M, Warrens BH, Jones PJ (2011) Rapid parallel evolution of aberrant traits in the diversification of the Gulf of Guinea white-eyes (Aves, Zosteropidae). *Mol Ecol* 20: 4953–4967.
90. Avise JC (2000) *Phylogeography: The History and Formation of Species*. Cambridge: Harvard University Press. 447 p.
91. Beebee TJC (2005) Conservation genetics of amphibians. *Heredity* 95: 423–427.
92. Jehle R, Wilson GA, Arntzen JW, Burke T (2005) Contemporary gene flow and the spatio-temporal genetic structure of subdivided newt populations (*Triturus cristatus*, *T. marmoratus*). *J Evol Biol* 18: 619–628.
93. Taylor EH (1968) *The caecilians of the world: a taxonomic review*. Lawrence: University of Texas Press.
94. Presswell B (2002) *Morphological and molecular systematic studies of Asian caecilians (Amphibia: Gymnophiona)*. PhD thesis. Scotland: University of Glasgow.
95. Gower DJ, Dharme M, Bhatta G, Giri V, Vyas R, et al. (2007) Remarkable genetic homogeneity in unstriped, long-tailed *Ichthyophis* along 1500 km of the Western Ghats, India. *J Zool* 272: 266–275.
96. Nishikawa K, Matsui M, Yong HS, Ahmad N, Yambun P, et al. (2012) Molecular phylogeny and biogeography of caecilians from Southeast Asia (Amphibia, Gymnophiona, Ichthyophiidae), with special reference to high cryptic species diversity in Sundaland. *Mol Phylogenet Evol* 63: 714–723.
97. Hardy ME, Grady JM, Routman EJ (2002) Intraspecific phylogeography of the slender madtom: the complex evolutionary history of the Central Highlands of the United States. *Mol Ecol* 11: 2393–2403.
98. Janzen FJ, Krenz JG, Haselkorn TS, Brodie ED Jr, Brodie ED III (2002) Molecular phylogeography of common garter snakes (*Thamnophis sirtalis*) in western North America: implications for regional historical forces. *Mol Ecol* 11: 1739–1751.
99. Castoe TA, Chippindale PT, Campbell JA, Ammerman LK, Parkinson CL (2003) Molecular systematics of the middle American jumping pitvipers (genus *Atropoides*) and phylogeography of the *Atropoides nummifer* complex. *Herpetologica* 59(3): 420–431.
100. Doan TM, Castoe TA (2003) Using morphological and molecular evidence to infer species boundaries within *Proctoporus bolivianus* Werner (Squamata: Gymnophthalmidae). *Herpetologica* 59(3): 432–449.
101. Fuerst GS, Austin CC (2004) Population genetic structure of the prairie skink (*Eumeces septentrionalis*): nested clade analysis of post Pleistocene populations. *J Herpetol* 38(2): 257–268.
102. Fouquet A, Gilles A, Vences M, Marty C, Blanc M, et al. (2007) Underestimation of species richness in neotropical frogs revealed by mtDNA analyses. *PLoS ONE* 2(10): e1109. doi:10.1371/journal.pone.0001109
103. Goldstien SJ, Dupont L, Viard F, Hallas PJ, Nishikawa T, et al. (2011) Global phylogeography of the widely introduced north west Pacific ascidian *Styela clava*. *PLoS ONE* 6(2): e16755. doi:10.1371/journal.pone.0016755
104. Levy E, Kennington WJ, Tompkins JL, LeBas NR (2012) Phylogeography and population genetic structure of the ornate dragon lizard, *Ctenophorus ornatus*. *PLoS ONE* 7(10): e46351. doi:10.1371/journal.pone.0046351
105. Milá B, Tavares ES, Muñoz Saldaña A, Karubian J, Smith TB, et al. (2012) A trans-Amazonian screening of mtDNA reveals deep intraspecific divergence in forest birds and suggests a vast underestimation of species diversity. *PLoS ONE* 7(7): e40541. doi:10.1371/journal.pone.0040541
106. Vences M, Thomas M, van der Meijden, Chiari Y, Vieites DR (2005) Comparative performance of the 16S rRNA gene in DNA barcoding of amphibians. *Front Zool* 2: 5. Available at <http://www.frontiersinzoology.com/content/2/1/5>